

of a stacking and close packing of these free radicals in rigid-rod polymer molecules. Long-range spin-spin interactions have, however, not been observed. Arguments to explain the absence of such coupling could be as follows:

There is the loss of approximately 20% of free radicals during synthesis, which could be detrimental for the magnetic properties.

According to McConnell's theory a negative value of the product of spin densities at two neighboring sites would predict ferromagnetism and a positive value antiferromagnetism (see refs 21 and 22). An exactly perpendicular

stacking would lead to a positive sign. Possibly, the stacking is not exactly perpendicular and the product of spin densities is vanishingly small.

**Acknowledgment.** We acknowledge the experimental support by H. W. van Kesteren and G. J. M. Poodt at Philips Research Laboratories, Eindhoven, and the recording of almost all NMR spectra by Dr. A. M. Kenwright, Department of Chemistry, University of Durham, UK.

**Registry No.** 2, 50432-01-4; 3, 134334-14-8; 3a, 134334-18-2; 4, 134334-15-9; 5, 134334-16-0; 5 (homopolymer), 134334-20-6; 6, 134334-17-1; 6 (homopolymer), 134334-21-7; 7 (SRU), 134334-23-9; 8 (SRU), 134334-24-0; HCO<sub>2</sub>H, 64-18-6; CH<sub>3</sub>COCl, 75-36-5.

(22) Izuoka, A.; Murata, S.; Sugawara, T.; Iwamura, H. *J. Am. Chem. Soc.* 1985, 107, 1786-1787.

## Aging Processes of Alumina Sol-Gels: Characterization of New Aluminum Polyoxycations by <sup>27</sup>Al NMR Spectroscopy

G. Fu and L. F. Nazar\*

*Department of Chemistry, University of Waterloo, Guelph-Waterloo Centre for Graduate Work in Chemistry, Waterloo, Ontario, Canada N2L 3G1*

A. D. Bain

*Department of Chemistry, McMaster University, Hamilton, Ontario, Canada L8S 4M1*

*Received September 7, 1990. Revised Manuscript Received March 19, 1991*

The existence of unidentified molecular aluminum oxide clusters has been previously postulated in many alumina sols produced by various methods. We have used <sup>27</sup>Al NMR spectroscopy kinetic studies to identify three new polyoxaluminum cations in these sols, which we show are formed by thermal transformation of the well-known tridecamer cation Al<sub>13</sub>O<sub>4</sub>(OH)<sub>24</sub>(H<sub>2</sub>O)<sub>12</sub><sup>7+</sup>. These clusters, which we denote as AIP<sub>1</sub>, AIP<sub>2</sub>, and AIP<sub>3</sub>, have resonances at 64.5 ppm (tetrahedral Al site)/≈10 ppm (octahedral Al site), 70.2 ppm (tet)/10.0 ppm (oct), and 75.6 ppm (tet)/9.3 ppm (oct), respectively. NMR and gel permeation chromatography data suggest that the poly(oxyaluminum) cation AIP<sub>2</sub>, which dominates this reaction process, is a dimer of Al<sub>13</sub>. A mechanism for the aging process is proposed.

### Introduction

Alumina sol-gels are complex, multicomponent fluids that are precursors for many materials such as controlled-porosity ceramic membranes, refractory fibers, coatings,<sup>1</sup> and optical matrices.<sup>2</sup> They are commonly formed from the hydrolysis of aluminum alkoxides, but they can also be produced by the polymerization of hydrated aluminum cations. The chemistry of these systems is still poorly defined, despite many years of study. We do know, however, that the nature of the elementary alumina species defines the bonding and microstructure in the sol. Given the importance of alumina sol-gel chemistry, this has motivated our studies to gain a fundamental understanding of the processes that control chemical composition and microstructure.

Past studies in this laboratory have centered on the alkoxide hydrolysis process. We have recently determined that the hydrolysis of aluminum alkoxides at high H<sub>2</sub>O/Al ratios at elevated temperature leads to the formation of small colloidal particles of aluminum hydroxyoxide linked

together to form an open, tenuous fractal structure.<sup>3</sup> The acid/Al ratio determines the degree of compactness of the network. Our small-angle neutron scattering experiments have revealed that the subunits of this fractal network are about 10-25 Å in diameter. Previous work has also shown that at room temperature, hydrolysis at high acid/Al ratios leads to the formation of alumina sols in which the Al<sub>13</sub>O<sub>4</sub>(OH)<sub>24</sub>(H<sub>2</sub>O)<sub>12</sub><sup>7+</sup> cation accounts for about 70% of the aluminum present.<sup>4,5</sup> We observed that aging these sols at 90 °C produced an unidentified species before gelation of the sol occurred. This molecule had a characteristic <sup>27</sup>Al NMR resonance at 70 ppm to high frequency (downfield) from Al(H<sub>2</sub>O)<sub>6</sub><sup>3+</sup>. In an effort to characterize this species and to better understand the steps in the aging and gelation process, we turned to the hydrolysis of aluminum salts in solution as a method of forming more characterizable sols.

At low pH (<3), aluminum salts exist in aqueous solutions as the hydrated Al<sup>3+</sup> cation. An increase in pH leads to the removal of H<sup>+</sup> from the coordinated water mole-

(1) Birchall, J. D. In *Fabrication Science 3*; Taylor, D., Ed.; British Ceramics Society: 33, Shelton, Stoke-on-Trent, U.K., 1983.

(2) Kobayashi, Y.; Kurokawa, Y.; Imai, Y.; Muto, S. *J. Non-Cryst. Solids* 1988, 105, 198.

(3) Nazar, L. F.; Klein, L. C. *J. Am. Ceram. Soc.* 1988, 71, C85.

(4) Nazar, L. F.; Klein, L. C.; Napier, D. C. *Better Ceramics Through Chemistry III. Mat. Res. Soc. Symp. Proc.* 1988, 121, 133.

(5) Nazar, L. F.; Napier, D. C.; Lapham, D.; Epperson, J. E. *Better Ceram. Chem. IV, Symp.* 1990, 180, 117.

cules, followed by condensation of the OH groups. Ultimately, this hydrolysis process leads to growth of large colloidal species and the formation of sol-gels. The reaction of aluminum salts with base has been studied for more than half a century<sup>6-8</sup> by using potentiometric titration,<sup>9</sup> ferron reaction kinetic studies,<sup>10,11</sup> small-angle X-ray scattering,<sup>12,13</sup> gel permeation chromatography (GPC),<sup>8,14,15</sup> and most recently <sup>27</sup>Al NMR spectroscopy.<sup>16-24</sup> Many species,  $Al_p(OH)_q^{(3p-q)+}$ , with different polymerization degrees,  $p$ , and different internal hydrolysis ratios,  $q/p$ , have been reported in this complex system. However, only a few of them have been unambiguously identified, namely, the monomer  $Al(H_2O)_6^{3+}$ , its hydrolysate<sup>23</sup>  $Al(OH)^{2+}$ , and the tridecamer  $Al_{13}O_4(OH)_{24}(H_2O)_{12}^{7+}$  ( $Al_{13}$ ). The structure of  $Al_{13}$ , which is one of the well-known Keggin isomers, has been determined by X-ray crystallography.<sup>25</sup> The same structure has been shown to exist in solution by comparison of the solution- and solid-state <sup>27</sup>Al NMR spectra.<sup>26,27</sup> The dimeric cation species,  $Al_2(OH)_2(H_2O)_8^{4+}$ , which has been crystallized as the sulfate salt,<sup>28</sup> was thought to be the source of a broadened NMR resonance at about 4 ppm in hydrolyzed aluminum solutions. However, recent evidence suggests the species responsible is a trimer, either  $Al_3(OH)_4^{5+}$  (potentiometric studies)<sup>9</sup> or  $Al_3(OH)_8^+$  (NMR spectroscopy).<sup>21</sup>

It is commonly believed that one or several other polycation species also exist in highly neutralized aluminum solutions ( $OH/Al > 2.5$ ), in addition to the  $Al_{13}$  cluster. The existence of an aluminum octamer,  $Al_8(OH)_{20}^{4+}$ , has been postulated, although no direct evidence exists for its formation. Akitt et al. reported the observation of an "Al<sub>13</sub>-like" species in prolonged Al metal hydrolyzed and aged base-hydrolyzed solutions, characterized by a broad resonance in the tetrahedrally coordinated aluminum region at about 70 ppm.<sup>16,17,21</sup> The same resonance at 70 ppm was reported by Muller et al.<sup>29,30</sup> and more recently by

Wood and co-workers in  $AlCl_3$ /urea hydrolyzed sols.<sup>24</sup> Turner<sup>10</sup> and Hsu<sup>11</sup> also separately described the observations of an unidentified polynuclear species in their studies of long-term aging (several years) at room temperature. The dilute, OH-hydrolyzed solution was analyzed by ferron kinetic methods. The unknown species was found to be much more resistant to attack by acids and ferron reagents than  $Al_{13}$ . A similar unknown species was also observed in the solution of aluminum chlorohydrate (ACH) by Fitzgerald<sup>8</sup> and in highly concentrated basic aluminum chloride solutions by Muller and co-workers.<sup>31,32</sup> Gel permeation chromatography on these solutions revealed two polymeric species with molecular weight ranges of 1500–3000 and 5000–8000 Daltons.<sup>8</sup>

This work was aimed at characterizing these unknown species by using high-field <sup>27</sup>Al NMR spectroscopy to follow the thermal evolution of the  $Al_{13}$  polycation. Here, we report on the isolation and <sup>27</sup>Al NMR study of one of these unidentified polynuclear species which has a characteristic NMR resonance at 70.2 ppm. Our results suggest that it arises from the condensation of two defect- $Al_{13}$  clusters. In addition, we have identified, for the first time, two new alumina sol clusters characterized by resonances in the tetrahedral Al region at 75.6 and 64.5 ppm and octahedral resonances at 9.3 and about 10 ppm. The former has been isolated by GPC.

## Experimental Section

Hydrolysis experiments were performed by adding either sodium carbonate or sodium hydroxide solutions to  $AlCl_3 \cdot 6H_2O$  solutions at ambient or elevated temperatures or by the reaction of aluminum foil with aluminum chloride solutions at 60–95 °C. In the case of Al metal hydrolysis, when the temperature was lower than 60 °C, mercury was occasionally added to speed up the reaction. The hydrolysis ratio,  $m = OH/Al$ , was calculated by using the following equation:

$$m = 3Y/(1 + Y)$$

where  $Y$  is the moles of Al foil per mole of  $AlCl_3$ .<sup>17</sup>

To prepare the  $Al_{13}$  solutions for these aging studies, the cation was first crystallized as the sulfate salt by using a modified literature method.<sup>25</sup> A 0.1 M  $AlCl_3$  solution was rapidly neutralized to  $m = 2.46$  at 90–100 °C with vigorous stirring. While the solution was still hot, a 10-fold excess of sodium sulfate (0.2 M solution) was added, and the cloudy precipitate that formed immediately was filtered off. The filtrate was cooled slowly, and small tetrahedral crystals of  $Na[AlO_4(OH)_{24}(H_2O)_{12}][SO_4]_4$  formed on the beaker walls after a few days. The identity of the crystals was confirmed by the match of their X-ray diffraction pattern to that reported previously<sup>11</sup> and also by their FT-IR and <sup>27</sup>Al MAS NMR spectra. The  $Al_{13}$  solution was then obtained by a metathesis reaction with  $BaCl_2$ .<sup>33</sup> The  $Al_{13}$  sulfate (0.5 g) was added to 10 mL of a 0.3 M  $BaCl_2$  solution, and after this stirred for 3–4 h, the solid  $BaSO_4$  was filtered off. Atomic absorption and <sup>27</sup>Al NMR analysis showed that the  $Al_{13}$  cation is the only aluminum-containing species present in the filtrate.

<sup>27</sup>Al NMR spectra were obtained on a Bruker AM-500 spectrometer operating at 130.3 MHz using a 10-mm VSP probe, with a sweep width of 50 kHz. Typically, 500–3000 free induction decays were accumulated at a repetition time of 1 s, with no acquisition delay. Under these conditions, spectrometer dead time can affect the integrated intensities of very broad lines by up to 20%. Aging of the solution at 85 °C was carried out in the probe

(6) Baes, C. F., Jr.; Messmer, R. E. In *The hydrolysis of cations*; John Wiley and Sons: New York, 1978.

(7) Akitt, J. W. *Prog. Nucl. Magn. Reson. Spectrosc.* 1989, 21, 1.

(8) Fitzgerald, J. J. In *Antiperspirants and Deodorants*; Laden, K., Felge, C., Eds.; Dekker: New York, 1988; pp 119–291.

(9) Brown, P. L.; Sylva, R. N.; Batley, G. E.; Ellis, J. J. *Chem. Soc., Dalton Trans.* 1985, 1967.

(10) Turner, R. T. *Can. J. Chem.* 1976, 54, 1528; *Ibid.* 1976, 54, 1910.

(11) Tsai, P. P.; Hsu, P. H. *J. Am. Soil Sci. Soc.* 1984, 48, 59; *Ibid.* 1985, 49, 1060.

(12) Axelos, M.; Tchouber, D.; Bottero, J. Y.; Fiessinger, F. *J. Phys.* 1985, 46, 1587.

(13) Bottero, J. Y.; Axelos, M.; Tchouber, D.; Cases, J. M.; Fripiat, J.; Fiessinger, F. *J. Colloid Interface Sci.* 1987, 117, 47.

(14) Akitt, J. W.; Farthing, A. J. *Chem. Soc., Dalton Trans.* 1981, 1606.

(15) Schonherr, V. S.; Frey, H. P. *Z. Anorg. Allg. Chem.* 1979, 452, 167.

(16) Akitt, J. W.; Mann, B. E. *J. Magn. Reson.* 1981, 44, 584.

(17) Akitt, J. W.; Farthing, A. J. *Chem. Soc., Dalton Trans.* 1981, 1617, 1624.

(18) Akitt, J. W.; Gessner, W. *J. Chem. Soc., Dalton Trans.* 1984, 147.

(19) Thompson, A. R.; Kunwar, A. C.; Gutowsky, H. S.; Oldfield, E. *J. Chem. Soc., Dalton Trans.* 1987, 2317.

(20) Akitt, J. W.; Elders, J. M. *J. Chem. Soc., Dalton Trans.* 1988, 1347.

(21) Akitt, J. W.; Elders, J. M.; Fontaine, X. L. R.; Kundu, A. K. *J. Chem. Soc., Dalton Trans.* 1989, 1889.

(22) Fitzgerald, J. J.; Johnson, L. E.; Frye, J. S. *J. Magn. Reson.* 1989, 84, 121.

(23) Akitt, J. W.; Elders, J. M. *J. Chem. Soc., Faraday Trans. 1* 1985, 81, 1923.

(24) Wood, T. E.; Siedle, A. R.; Hill, J. R.; Skarjune, R. P.; Goodbrake, C. *J. Better Ceram. Chem. IV, Symp.* 1990, 180, 97.

(25) Johansson, G. *Acta Chem. Scand.* 1960, 14, 769, 771.

(26) Muller, D.; Gessner, W.; Schonherr, S.; Gorz, H. *Z. Anorg. Allg. Chem.* 1981, 483, 153.

(27) Kunwar, A. C.; Thompson, A. R.; Gutowsky, H. S.; Oldfield, E. *J. Magn. Reson.* 1984, 60, 467.

(28) Johansson, G. *Acta Chem. Scand.* 1962, 16, 403.

(29) Schonherr, S.; Gorz, H.; Gessner, W.; Winzer, M.; Muller, D. *Z. Anorg. Allg. Chem.* 1981, 476, 1985.

(30) Schonherr, S.; Gorz, H.; Bertram, R.; Muller, D.; Gessner, W. *Z. Anorg. Allg. Chem.* 1983, 502, 113.

(31) Bertram, R.; Gessner, W.; Muller, D.; Gorz, H.; Schonherr, S. *Z. Anorg. Allg. Chem.* 1985, 525, 14.

(32) Bertram, R.; Gessner, W.; Muller, D. *Z. Chem.* 1986, 26, 342.

(33) Schonherr, S.; Gorz, H.; Muller, D.; Gessner, W. *Z. Anorg. Allg. Chem.* 1981, 467, 188.

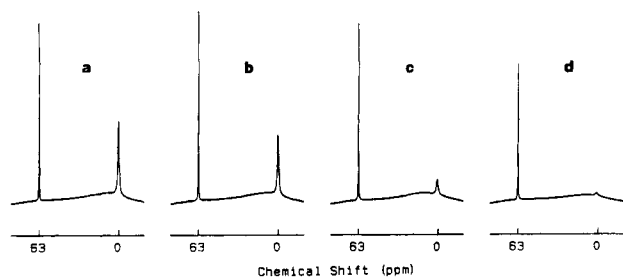


**Figure 1.**  $^{27}\text{Al}$  NMR spectra at 52.1 MHz and 85 °C of  $\text{AlCl}_3 \cdot (\text{H}_2\text{O})_6$  hydrolyzed by  $\text{OH}^-$  [ $\delta$  relative to external  $[\text{Al}(\text{H}_2\text{O})_6]^{3+}$ ]. The degree of hydrolysis is indicated by  $m$  (see text); (a)  $m = 2.25$ ; (b)  $m = 2.35$ ; (c)  $m = 2.45$ ; (d)  $m = 2.55$ .

of the spectrometer at aging times up to 40 h; a spectrum was recorded every 2 h. Samples were heated in an oven at 85 °C for aging periods that exceeded 40 h. In a few cases (noted in the figures), spectra were recorded on a Bruker AM-200 spectrometer operating at 52.1 MHz. Chemical shifts have been reported relative to 1 M  $[\text{Al}(\text{H}_2\text{O})_6]^{3+}$ , which was used as an external standard. The chemical shift values and line widths were determined from computer simulation of the spectra by using least-squares curve-fitting procedures based on a Simplex routine, performed on a IBM-compatible PC using the program NMR-286 (Dr. T. Allman, SoftPulse Software, 1989). The NMR peaks were approximated by using Lorentzian line shapes.

Gel permeation chromatography was carried out using a  $90 \times 2.8$  cm column packed with a polyacrylamide gel, Bio-Gel-P2, which has the fractionation range of 100–1800 Daltons for globular biomolecules. The 8-mL sample was eluted with Millipore water at a flow rate of 44 mL/h. A total of 80 fractions were collected for each run. Selected fractions were analyzed by  $^{27}\text{Al}$  NMR, and total aluminum was analyzed by atomic absorption spectroscopy.

## Results

**OH/Al Ratio-Dependent Hydrolysis.** The nature of the species formed in the alumina sol is determined by four reaction parameters: the OH/Al ratio ( $m$ , or neutralization ratio), the Al concentration, and the aging time and temperature. The Al concentration does not greatly influence the outcome of hydrolysis unless the solution is extremely dilute ( $<10^{-4}$  M)<sup>13</sup> or very concentrated ( $>1.5$  M).<sup>8,29,30</sup> As our studies have been carried out in the intermediate range of 0.1–1.5 M Al, this factor is not significant here. In addition, we limited our studies to an OH/Al ratio range of  $m = 2.0$ – $2.6$ , where the unknown poly(oxylation) species are known to exist.

Figure 1 shows the solution spectra of  $\text{AlCl}_3$  hydrolyzed with 0.2 M NaOH at room temperature, to  $m = 2.25$ , 2.35, 2.45, and 2.55. It can be seen that when  $m > 2.40$ , the  $\text{Al}_{13}$  decays and changes into other species that are invisible by NMR even at 85 °C. Thus, we conclude that simply increasing the hydrolysis ratio does not produce any new, NMR-observable species.

When the hydrolysis was carried out by the reaction of Al metal with  $\text{AlCl}_3$  solutions for 60 h at 85 °C at the same  $m$  ratios, the spectra obtained were quite different. These are shown in Figure 2. Two new resonances are evident in these spectra in the tetrahedral region at 70.2 and 75.6 ppm, and a resonance in the octahedral region at about 10 ppm is readily observable. The peak at 70.2 ppm has been observed previously by others under similar conditions.<sup>17,21</sup> These differences can be attributed to the prolonged hydrolysis time at elevated temperature and the increased Al concentration in the solution. Thus, the hydrolysis process is also an aging process for those species formed long before the Al metal hydrolysis reaction is complete.

The most important feature of the spectra in Figure 2 is that the ratio of the 70 ppm species to  $\text{Al}_{13}$  is not greatly

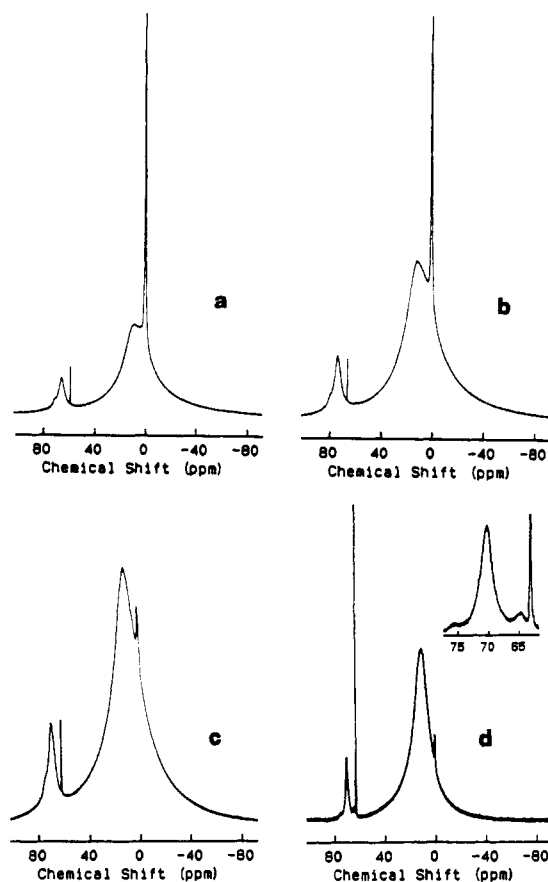


**Figure 2.**  $^{27}\text{Al}$  NMR spectra at 85 °C of  $\text{AlCl}_3 \cdot (\text{H}_2\text{O})_6$  hydrolyzed by reaction with Al foil; (a)  $m = 2.25$ ,  $t = 60$  h; (b)  $m = 2.35$ ,  $t = 60$  h; (c)  $m = 2.45$ ,  $t = 60$  h; (d)  $m = 2.45$ ,  $t = 15$  h. Inset shows expansion in the tetrahedral region. Spectra a–c are recorded at 52.1 MHz; spectrum d is recorded at 130.3 MHz.

affected by the hydrolysis ratio in the range studied. However, the aging time strongly affects speciation. At shorter aging periods (15 h), the spectrum of a metal-hydrolyzed solution at the same hydrolysis ratio shows another  $T_d$  resonance at 64.5 ppm, in addition to the peaks at 70.2 and 75.6 ppm (Figure 2d). We have found that the 64.5 ppm resonance is observable only when the reaction time is short, but the 75.6 ppm species is prominent only at very long reaction times. The independence of the intensity changes of these new resonances in the tetrahedral region indicates that they represent three distinct poly(oxyaluminum) cations.

**High-Temperature Aging of an  $\text{Al}_{13}$  Solution.** The evidence obtained from the above studies suggests that the aging products were produced from transformation of the  $\text{Al}_{13}$  cluster on thermal treatment. However, we know that in these systems that there may be hydrolysis products that are not observable by  $^{27}\text{Al}$  NMR spectroscopy, due to either a large quadrupole coupling or a high molecular weight. Hence, NMR-invisible species could also be precursors of the new species. This makes the interpretation of the NMR spectra very difficult. To simplify the problem, we chose a system that initially contains only the  $\text{Al}_{13}$  cations in solution. This was prepared by a metathesis reaction as previously described.

Figure 3 shows the spectral developments on aging the pure  $\text{Al}_{13}$  solution (Figure 3a) in the NMR probe at 85 °C for 38 h (Figure 3b–g). Continued heating of the 38-h-aged solution in an oven at 85 °C for an additional 42 h (total 80 h) and an additional 50 h (total 130 h) gave the spectra shown in Figure 3h,i, respectively. It is clearly seen that aging results in decay of the tetrahedral resonance of  $\text{Al}_{13}$

Table I. Integrated Intensities of the  $^{27}\text{Al}$  NMR Resonances for Selected Spectra Shown in Figure 3

time, h	integrated intensities for alumina species (arbitrary units)			sum of contributions from $\text{AIP}_1 + \text{AIP}_2$		
	0 ppm <sup>a</sup> ( $\text{Al}^{3+}$ )	62.9 ppm <sup>a</sup> ( $\text{Al}_{13}$ )	$\sim 10$ ppm <sup>a</sup> (oct, total)	$T_d$ sites <sup>a</sup> (70.2 + 64.5 ppm)	$O_h$ sites <sup>b</sup>	$O_h/T_d$ ratio ( $\text{AIP}_1 + \text{AIP}_2$ )
2	0.8	29	359	6	64	10.4
6	2.1	26	375	10	115	11.1
12	3.0	21	393	15	180	11.7
18	3.7	17	396	20	230	11.4
24	4.6	13	402	24	271	11.3
30	4.8	11	401	26	294	11.2
38	5.2	8	396	28	315	11.2

<sup>a</sup> Obtained from least-squares curve fitting. Estimated error is 5–8%. <sup>b</sup> Obtained by subtracting the octahedral contribution for  $\text{Al}_{13}$  (10.2  $\times$  tetrahedral intensity) from the total octahedral resonance intensity at  $\sim 10$  ppm.

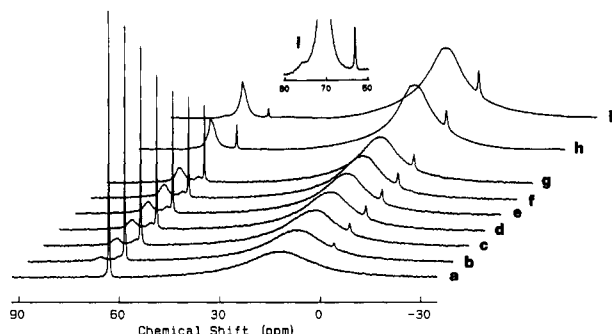
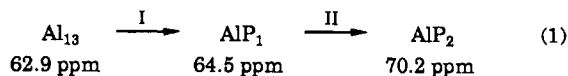


Figure 3.  $^{27}\text{Al}$  NMR spectra showing the thermal evolution of a 0.035 M solution of  $[\text{Al}_{13}\text{O}_4(\text{OH})_{24}(\text{H}_2\text{O})_{12}][\text{Cl}]_7$  at 85 °C. Spectra are recorded in situ at 130.3 MHz as a function of aging time: (a) 0; (b) 6; (c) 12; (d) 18; (e) 24; (f) 30; (g) 38; (h) 80; (i) 130 h. Inset shows expansion in the tetrahedral region.

at 62.9 ppm. This is accompanied by the growth of two new peaks in the tetrahedral region at 64.5 (“ $\text{AIP}_1$ ”), and at 70.2 ppm (“ $\text{AIP}_2$ ”), in addition to a resonance at 0 ppm corresponding to the monomer ( $\text{Al}(\text{H}_2\text{O})_6^{3+}$ ). These results suggest that the  $\text{Al}_{13}$  disproportionates into  $\text{AIP}_n$  and  $\text{Al}^{3+}$ . The  $\text{AIP}_1$  resonance at 64.5 ppm remains throughout the early stages of the aging process and then begins to slowly decay after about 80 h of aging. To obtain quantitative information about the changes in peak areas as a function of aging, computer simulations of the spectra in Figure 3 were performed. The results of the quantitative curve-fitting analysis are presented in Table I for aging up to 38 h. The data for the tetrahedral region are also shown in graphical form in Figure 4. The total peak area of the three tetrahedral resonances and hence the total number of tetrahedral sites remain constant in the aging process. Note that  $\text{AIP}_1$  is formed immediately at the beginning of the aging process and remains at a low but constant concentration.  $\text{AIP}_2$  is formed in subsequent steps in which its rate of increase correlates with the decay of  $\text{Al}_{13}$ . The decay of  $\text{Al}_{13}$  is first-order (or pseudo-first-order) with a rate constant of 0.036  $\text{h}^{-1}$ . We conclude that the transformation of  $\text{Al}_{13}$  to the two new species involves only the distortion of the tetrahedral aluminum sites and does not result in their loss. Furthermore,  $\text{AIP}_1$  seems to be an intermediate species in a process in which the rate of its generation roughly equals that of its consumption. We propose that the following transformation takes place:



The data in Table I show that the average ratio of the octahedral to tetrahedral sites in the two new species is close to 11. This value was calculated by subtracting the octahedral site  $\text{Al}_{13}$  contribution from the total octahedral

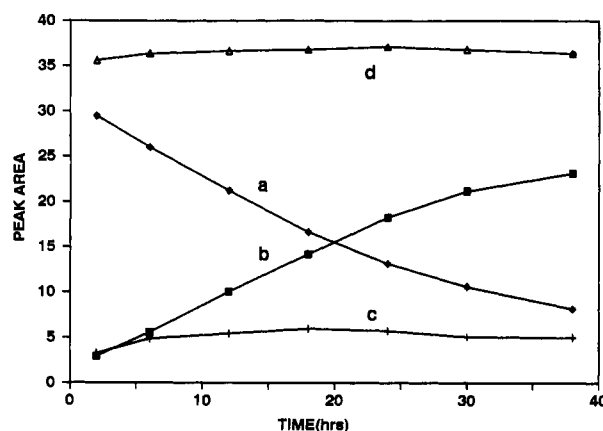
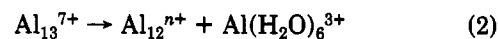


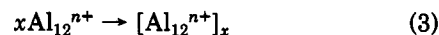
Figure 4. Changes in the areas of the tetrahedral NMR resonances from the experiment described in Figure 3b–g, as a function of aging time: (a) 62.9 ppm,  $\text{Al}_{13}$ ; (b) 70 ppm,  $\text{AIP}_2$ ; (c) 64.5 ppm,  $\text{AIP}_1$ ; (d) sum of a–c.

sites. The octahedral site  $\text{Al}_{13}$  value was calculated by multiplying the tetrahedral site area by 10.2, which was the experimentally determined ratio of octahedral/tetrahedral sites for the pure tridecamer at 85 °C. This ratio is in good agreement with that obtained for  $\text{Al}_{13}$  by others.<sup>19</sup> The ratio will be lower than expected, because signal intensity is lost in the broad octahedral resonance due to both spectrometer dead time and difficulties in distinguishing signal from the baseline in the spectrum. A loss of signal intensity for the octahedral sites in the new  $\text{AIP}_n$  species would not be expected to the same extent as in  $\text{Al}_{13}$ , because the quadrupole broadening in the octahedral sites is substantially less. This is evident from the line narrowing of the octahedral resonance during the aging period and was confirmed by subsequent experiments (vide infra). Thus, we are confident that this ratio of 11 determined by NMR reflects the actual site occupancy in the new polycation species.

Since monomer is generated in the aging process and its amount increases with aging time, it is reasonable to consider that the first step of reaction 1 involves the degradation of  $\text{Al}_{13}$ :



The unsaturated cluster  $\text{Al}_{12}^{n+}$  arising from the loss of one octahedral Al unit from the tridecamer cluster would have a structure comprised of one tetrahedral Al site and 11 octahedral sites. This, we propose, is the identity of  $\text{AIP}_1$ . The defect creates four active sites on  $\text{AIP}_1$  that can react by condensation/polymerization to form larger, more stable polycation species, i.e.,  $\text{AIP}_2$ :



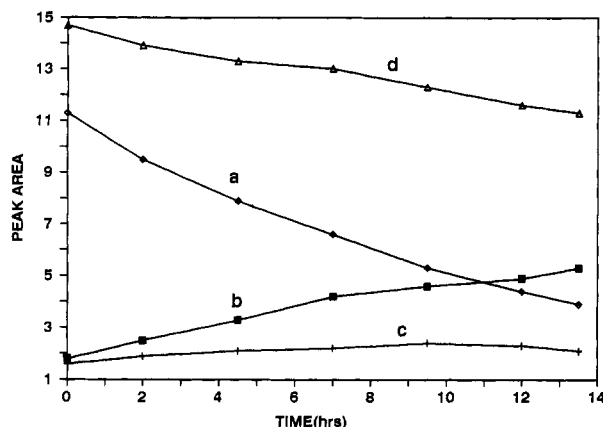


**Figure 5.** Aging of a solution of  $[\text{Al}(\text{H}_2\text{O})_6][\text{Cl}]_6$  hydrolyzed by  $\text{CO}_3^{2-}$  at  $85^\circ\text{C}$ . Areas of tetrahedral NMR resonances are shown as a function of aging time: (a)  $\text{Al}_{13}$ , 62.9 ppm; (b)  $\text{AlP}_2$ , 70 ppm; (c)  $\text{AlP}_1$ , 64.5 ppm; (d) sum of a-c.

The most probable value of  $x$  is 2. This is supported by our GPC results (vide infra) and those of others.<sup>8</sup> Possible structures of this species will be discussed in detail in the next section.

Interestingly, aging for more than 80 h (Figure 3h,i) results in complete loss of  $\text{AlP}_1$  and growth of another new resonance ( $\text{AlP}_3$ ) at 75.6 ppm. The appearance of this molecule at this stage suggests that its results from transformation of  $\text{AlP}_2$ .

**High-Temperature Aging of Carbonate-Hydrolyzed Solutions.** Hydrolysis of an  $\text{AlCl}_3$  solution by reaction with  $\text{NaCO}_3$ , as reported by Akitt,<sup>17</sup> gave an  $\text{Al}_{13}$  solution that had a spectrum identical with that obtained above. However, quantitative analysis of the spectra obtained during a 40-h heating period of these solutions (at  $85^\circ\text{C}$ ) showed that the aging behavior was different. The changes in peak areas in the tetrahedral region are summarized in Figure 5. The rate of decay of  $\text{Al}_{13}$  ( $0.078\text{ h}^{-1}$ ) is about twice that in the "pure" solution. The rate of increase of the tetrahedral resonance of  $\text{AlP}_2$  is substantially lower, which results in a decrease of the total area of the three tetrahedral resonances. In addition, although the observed NMR changes in the octahedral region were similar to those of the pure  $\text{Al}_{13}$  solution, the total peak area (not shown) also decreased during aging. This suggests that a portion of the  $\text{Al}_{13}$  polycations are transformed into NMR-invisible species in this process.

The differences are attributable to inhomogeneity in the  $\text{Na}_2\text{CO}_3$ -hydrolyzed sol, compared to the  $\text{Al}_{13}$  solution generated by metathesis. This is probably due to the formation of small amounts of colloidal particles that are NMR-invisible, which result from high local transient concentrations of hydroxide ion in this reaction. These act as nucleation sites for the crystallization of  $\text{Al}(\text{OH})_3$ . Accordingly, precipitation of pseudoboehmite was observed for both carbonate and Al metal-hydrolyzed solutions when the solutions were aged at  $85^\circ\text{C}$  for 2 weeks. These results agree with conclusions on pathways of gibbsite crystallization from hydrolyzed Al solutions.<sup>34</sup>

**$\text{AlP}_2$  Formation and Isolation.** We found that Al metal hydrolysis of  $\text{AlCl}_3$  solutions at elevated temperature was the best, direct method of preparing large amounts of  $\text{AlP}_2$ , as opposed to the thermal treatment of  $\text{Al}_{13}$ . We observed that the formation of  $\text{AlP}_2$  is favored at relatively high concentrations of  $\text{Al}_{13}$ , but if the concentration is too high, larger polymeric species may form. This is the case in aluminum chlorohydrate solutions.<sup>8</sup>

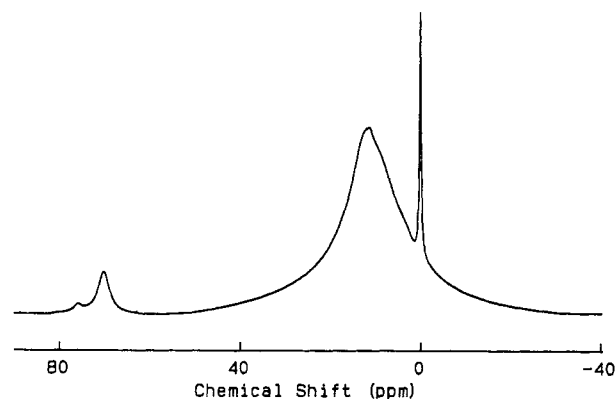


**Figure 6.**  $^{27}\text{Al}$  NMR spectra at  $85^\circ\text{C}$  of  $\text{AlCl}_3 \cdot (\text{H}_2\text{O})_6$  hydrolyzed by reaction with Al foil for 60 h at  $95\text{--}100^\circ\text{C}$ .

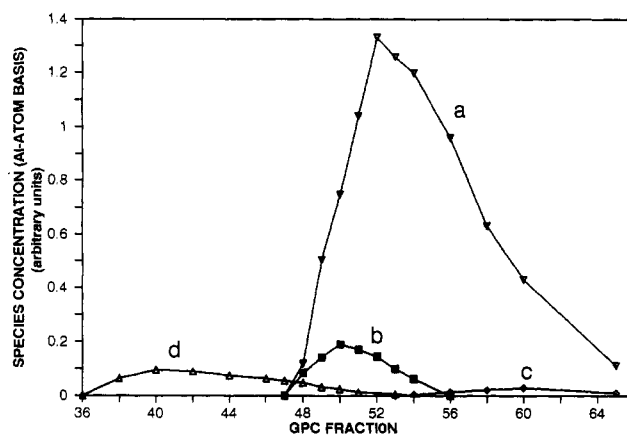


**Figure 7.** GPC elution profiles of the various alumina species: (a)  $\text{AlP}_2$ ; (b)  $\text{AlP}_3$ ; (c)  $\text{Al}_{13}$ ; (d)  $\text{Al}(\text{H}_2\text{O})_6^{3+}$ . The relative amounts of the first three species on an aluminum-atom basis were calculated from determination of the area of the tetrahedral ( $T_d$ ) resonance. The theoretical or experimentally determined octahedral contribution was then added to this value ( $12 \times T_d$ ,  $\text{Al}_{13}$ ;  $11 \times T_d$ ,  $\text{AlP}_2$ ;  $8.4 \times T_d$ ,  $\text{AlP}_3$ ).

For short metal-hydrolysis periods, a relatively large amount of  $\text{Al}_{13}$  is obtained together with the  $\text{AlP}_2$  species and a small amount of  $\text{AlP}_1$ . Most of the  $\text{Al}_{13}$  can be removed by prolonged hydrolysis, but the contamination of  $\text{AlP}_3$  becomes significant. Experimentally, we found that the optimum conditions for  $\text{AlP}_2$  preparation were hydrolysis at  $95\text{--}100^\circ\text{C}$  for 50–60 h. Figure 6 shows the spectrum of a typical solution that was obtained under these conditions with a total Al concentration of 1.35 M. Almost all the  $\text{Al}_{13}$  species has transformed into other poly(oxyaluminum) species, and about 90% of the tetrahedral aluminum is present as  $\text{AlP}_2$ . Atomic absorption analysis (AAA) together with calibration of the  $^{27}\text{Al}$  NMR spectrum with a solution of  $[\text{Al}(\text{H}_2\text{O})_6]^{3+}$  of known concentration indicated that a total of 94% of the aluminum was visible in the spectrum at  $85^\circ\text{C}$ .

Given that a pure solution of one polycation species cannot be obtained directly from hydrolysis, we turned to gel permeation chromatography to separate and isolate the molecules. Other work on GPC of hydrolyzed aluminum solutions,<sup>14,15</sup> in particular that of Fitzgerald,<sup>8</sup> has reported the use of the Sephadex G series chromatographic gels (mostly G-25). These gels worked very well in separating  $\text{Al}_{13}$  from very large polymeric species (MW range 5000–8000 Daltons), but they cannot differentiate between species that have a size and molecular weight comparable to  $\text{Al}_{13}$ . We had success, however, with Bio-Gel-P2, which is a polyacrylamide with a fractionation range of 100–1800

(34) Hsu, P. H. *Clays Clay Miner.* 1988, 36, 25.

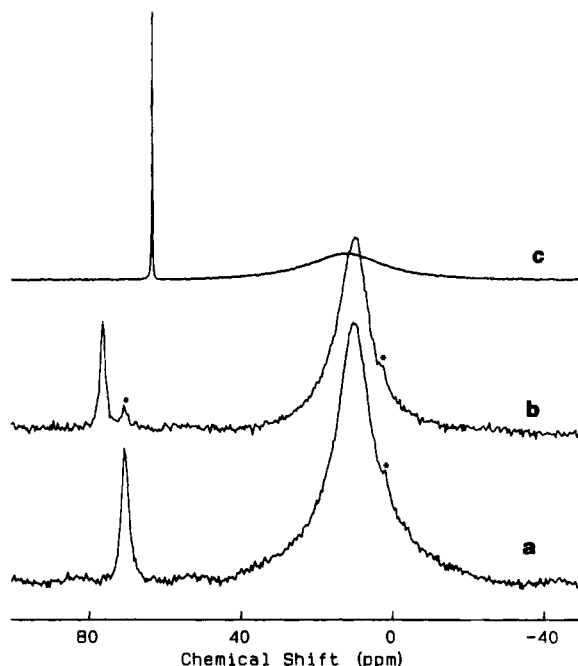


**Figure 8.**  $^{27}\text{Al}$  NMR spectra at 85 °C and 130.3 MHz, of solutions resulting from GPC isolation of (a)  $\text{AlP}_2$ ; (b)  $\text{AlP}_3$ ; (c)  $\text{Al}_{13}$ . Traces of  $\text{Al}(\text{H}_2\text{O})_6^{3+}$  (\*) are apparent in spectra a and b; some  $\text{AlP}_2$  (O) is also visible in spectrum (b).

Daltons. The solution shown in Figure 6 was used as the column charge.

Figure 7 shows the complete elution profile on Bio-Gel-P2 based on the relative amount (determined on an Al atom basis) of the polycation species and the monomer derived from curve fitting the NMR spectra of the fractions. A small amount (roughly 5% of the total Al) of an alumina species eluted in fractions 15–23, which was detected by AAA, but these fractions gave no observable NMR spectrum and thus presumably contain high-molecular-weight colloids. The three polycation species elute in the order  $\text{AlP}_3$ ,  $\text{AlP}_2$ ,  $\text{Al}_{13}$ . This implies that the size also decreases in this order, assuming, as we would expect, that the interaction with the gels are similar for these species.

The changes in the spectra from the GPC elution profile show that the three tetrahedral resonances belong to different species. This cannot be readily determined from the complex solution spectrum. Furthermore, it is possible to achieve a reasonable degree of separation by using this method. In particular,  $\text{AlP}_3$  could be isolated from  $\text{AlP}_2$  by repeating the column chromatography on the combined fractions containing high concentrations of these species. The NMR spectra that resulted are shown in Figure 8a,b, together with the NMR spectrum of a pure sample of  $\text{Al}_{13}$  for comparison (Figure 8c). The spectra were recorded at 90 °C. Fraction 35 contains  $\text{AlP}_2$  with a trace of monomer (Figure 8a): fraction 29 contains the  $\text{AlP}_3$  species, with traces of monomer and  $\text{AlP}_2$  (Figure 8b).

**$^{27}\text{Al}$  NMR Parameters of the Poly(oxaluminum) Clusters.** The  $^{27}\text{Al}$  NMR parameters of the four aluminum polycation species are summarized in Table II. These data were obtained from curve fitting of the spectra shown in Figures 3 ( $\text{Al}_{13}$ ,  $\text{AlP}_1$ ) and 8a,b, ( $\text{AlP}_2$ ,  $\text{AlP}_3$ ).

The octahedral resonance of the  $\text{Al}_{13}$  cation is not readily observable at room temperature, as others have noted. This is the result of extremely fast spin relaxation caused by quadrupolar interaction with the electric field gradient at the asymmetric octahedral Al site. The resulting broad line narrows with increasing temperature, due to the effect

**Table II.**  $^{27}\text{Al}$  NMR Chemical Shift and Line-Width Data of Alumina Poly(oxycations)<sup>a</sup>

poly(oxo-cation)	T, K	tetrahedral sites		octahedral sites		$O_n/T_d$ ratio (obsd)
		$\delta_{\text{Al}}$ , ppm	$\Delta\nu_{1/2}$ , Hz	$\delta_{\text{Al}}$ , ppm	$\Delta\nu_{1/2}$ , Hz	
$\text{Al}_{13}$	358	62.9	20	11.8	2700	10.2 <sup>b</sup>
$\text{AlP}_1$	358	64.5	270			(11) <sup>c</sup>
$\text{AlP}_2$	363	70.2	318	10.0	1665	10.8
$\text{AlP}_3$	363	75.6	210	9.3	1290	8.4

<sup>a</sup> Obtained from curve-fitting (see text). <sup>b</sup> Theoretical value is 12 (see text). <sup>c</sup> Estimated value.

of the rotational correlation time on the quadrupolar relaxation rate. Hence, the solution NMR parameters of  $\text{Al}_{13}$  are dependent on experimental conditions, and few definitive assignments of the octahedral resonance have been made. Our value of the chemical shift of 11.8 ppm is close to the isotropic value of  $11 \pm 3$  ppm determined for crystalline  $\text{Al}_{13}$  in the solid state by variable-angle spinning,<sup>27</sup> although it differs from that reported by the same authors for the solution preparation by carbonate hydrolysis at  $m > 2$ .<sup>19</sup>

This is the first time that detailed NMR parameters are given for the other three species, although there have been many reports of the observation of the 70 ppm species and brief mention of the 75 ppm species.<sup>22</sup> Note that the octahedral/tetrahedral ratio measured for isolated  $\text{AlP}_2$  is indeed close to 11, as previously estimated in Table I. The tetrahedral resonances of  $\text{AlP}_{1,2,3}$  at 64.5, 70.2, and 75.6 ppm are all much broader than the tetrahedral  $\text{Al}_{13}$  resonance, which indicates that the electric field at the tetrahedral site in their structures is less symmetrical than that of the tridecamer. This is probably the result of structural site symmetry. Previous work has also determined that there is a direct correlation between chemical shift values and bond lengths in solid-state aluminates.<sup>35</sup> The successive increase of the chemical shifts of these peaks thus indicates that the bond lengths in the tetrahedral sites in  $\text{AlP}_1$ ,  $\text{AlP}_2$ , and  $\text{AlP}_3$  are on average, progressively shorter than that in the tridecamer. On the other hand, for the octahedral sites, the broad resonance at about 10 ppm is narrowed considerably by comparison to  $\text{Al}_{13}$ . Although these polycations are likely to have more than one type of octahedral site, at least some of the sites are clearly more symmetric than in the tridecamer (which has only one type of octahedral site). These changes in site electric field symmetry and bond lengths are significant but within the range of those values reported for other aluminate structures.<sup>27,35</sup>

In the case of rapid molecular tumbling in solution, where extreme motional narrowing occurs, the spin-lattice ( $T_1$ ) and spin-spin ( $T_2$ ) times should be equivalent.  $T_2$  can be calculated from the width of the NMR line at half-height, i.e.,  $T_2 = 1/\pi\Delta\nu_{1/2}$ . We find that  $T_2$  values of  $\text{AlP}_2$  for the octahedral and tetrahedral sites measured at 90 °C to be  $2.1 \times 10^{-4}$  and  $1.2 \times 10^{-3}$  s, respectively, in reasonably good agreement with our preliminary  $T_1$  measurements. Combining this information together with our estimated quadrupole coupling constant for the tetrahedral site for  $\text{AlP}_2$  of about 2 MHz,<sup>36</sup> we can use the Stokes-Einstein-Debye relationship to estimate the size of  $\text{AlP}_2$ .<sup>27,37</sup> We

(35) Muller, D.; Gessner, W.; Samoson, A.; Lippmaa, E.; Scheler, G. *J. Chem. Soc., Dalton Trans* 1986, 1277.

(36) The quadrupole coupling constant,  $e^2qQ/h$ , for the tetrahedral site was estimated from MAS NMR measurements of the second-order quadrupole-induced chemical shift on a sample of the  $\text{AlP}_2$  sulfate salt at 130.2, 104.2, and 78.2 MHz. Full details will be reported in a subsequent paper.



find the approximate value of the radius of this molecule to be about 7 Å, in good agreement with that expected for our dimeric structure (cf. the radius of  $\text{Al}_{13} = 5.4 \text{ \AA}$ ).

### Discussion

**Hydrolysis and Aging Mechanisms.** Our study sheds new light on many observations of both the early and late stages of hydrolysis of aluminum species in solution and suggests a sequence in the aging and growth of poly(oxyaluminum) clusters in alumina sols. In the early stages of hydrolysis, three species have been characterized by previous NMR studies, the monomer (0 ppm), the oligomer (ca. 4 ppm), and the tridecamer (62.9 ppm ( $T_d$ ), 11.8 ppm ( $O_h$ )). Although there are different opinions on the internal hydrolysis ratio of the oligomer species, it is well-known that this species dominates at an OH/Al ratio of  $m = 1$ . It also is in some way related to the well-known polycation species,  $\text{Al}_{13}$ , since it transforms into  $\text{Al}_{13}$  upon dilution.<sup>20</sup> From  $m = 1.5$  to  $m = 2.5$ ,  $\text{Al}_{13}$  is the dominant species.

In this work, we have shown that in aging a pure  $\text{Al}_{13}$  solution, the  $\text{Al}_{13}$  molecules gradually transform into a more stable species,  $\text{AlP}_2$ , through an intermediate species  $\text{AlP}_1$ . In this process, the tetrahedral sites are conserved, although the site symmetry is lowered as a result of bond length or bond angle changes. When a large majority (>90%) of the  $\text{Al}_{13}$  has been transformed into  $\text{AlP}_2$ , further aging leads to the transformation of  $\text{AlP}_2$  into another polycation species,  $\text{AlP}_3$ .

If the aging experiments are performed on an  $\text{Al}_{13}$  solution that contains aluminum hydroxide nuclei, e.g., a carbonate-hydrolyzed solution, two reaction paths account for the decay of  $\text{Al}_{13}$ . One is the same as the pure  $\text{Al}_{13}$  solution case described above, and the other is the direct transformation of  $\text{Al}_{13}$  into  $\text{AlOOH}$  or  $\text{Al}(\text{OH})_3$ . As discussed by Hsu, crystallization of aluminum hydroxide is probably started by the deposition of monomeric species, which dissociate from the  $\text{Al}_{13}$  polyoxocations onto the crystallite seeds present in solution.<sup>34</sup> In the latter case, the aging studies were carried out at room temperature, in which  $\text{Al}(\text{OH})_3$  is known to form. We do not know the nature of our amorphous aluminum hydroxyoxide that initially precipitates, although it is likely that this high-temperature aging process results in the ultimate formation of pseudoboehmite,  $\text{AlOOH}$ , by a similar mechanism. This is suggested by studies of aluminum alkoxide hydrolysis, in which boehmite has been proven to form from high-temperature (80–95 °C) processing, but bayerite,  $\text{Al}(\text{OH})_3$ , forms under room-temperature conditions.<sup>35</sup> Proof of the formation of boehmite in our system would indicate that this difference is mechanistically controlled.

In addition to the mechanism this paper has addressed, an additional pathway has been invoked by Botero et al. This was proposed on the basis of  $^{27}\text{Al}$  NMR and small-angle X-ray scattering studies of aluminum hydroxide formation from progressive neutralization of aluminum chloride solutions at room temperature. They have concluded that when the hydrolysis ratio is at about 2.3 that  $\text{Al}_{13}$  molecules begin to aggregate with progressive removal of  $\text{Cl}^-$  and adjacent octahedral hydroxyl groups condense into oxo bridges.<sup>13</sup> They determined that the Al tetrahedra are protected against the increasing  $\text{OH}^-$  concentration up to  $m = 2.8$ . When this limit is passed, they rearrange into octahedra, and for  $m = 3$ , the long-range order of bayerite is obtained.

A consistent picture that summarizes the hydrolysis and aging mechanisms based on these observations above is

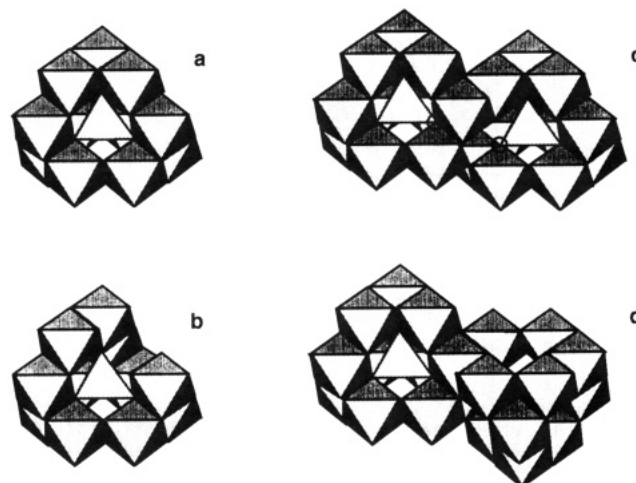
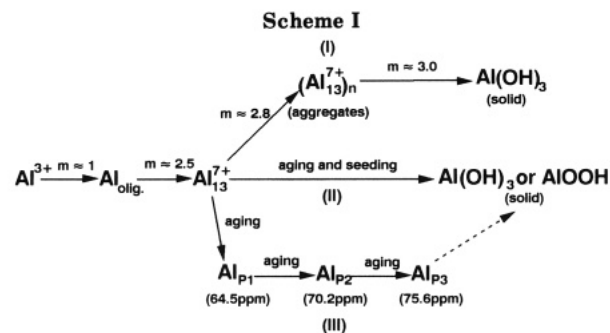


**Figure 9.** Structural models for the poly(oxyaluminum) cations: (a)  $\text{Al}_{13}$ ; (b)  $\text{AlP}_1$  "defect" structure showing loss of one octahedron from  $\text{Al}_{13}$ ; (c) a possible "unsaturated" structure for  $\text{AlP}_2$ , in which the tetrahedral Al site is coordinated to only 11 Al octahedra. In this structure, three of the oxygen atoms of the  $\text{AlO}_4$  tetrahedra are connected to three Al octahedra, and the fourth oxygen atom is connected to two Al octahedra (indicated by  $\text{O}$ ). (d) A "saturated" structure for  $\text{AlP}_2$  in which the tetrahedral Al site is fully coordinated to 12 Al octahedra.



shown in Scheme I. There are three transformation paths from  $\text{Al}_{13}$  to the solid hydroxide. We have provided direct evidence for path III. Path I is based on the study by Bottero and Cases.<sup>13</sup> Our NMR studies show, however (Figure 1), that  $\text{Al}_{13}$  begins to lose some tetrahedral resonance intensity at  $m = 2.45$ , which is earlier than they report ( $m = 2.8$ , path I).

**Structural Models for the Poly(oxyaluminum) Cations.** We observed in our NMR studies that the four polycation species exist in different stages of aging. We also believe that all of the three new species are derived from the original  $\text{Al}_{13}$  species (Scheme I, path III), and hence their structure must be related to that of the tridecamer. The structure of the  $\text{Al}_{13}$  polycation is well-known and has been shown to belong to one of the five Baker-Figgis isomers of the Keggin structure ( $\epsilon$ -structure, Figure 9a). The  $\alpha$ - and  $\beta$ -isomers of this structure are commonly found in heteropolyanions of molybdenum and tungsten.<sup>38</sup>

If one of the twelve peripheral octahedral Al atoms is removed from the structure together with its coordinated water, a defect Keggin structure is obtained (Figure 9b). This is the structural model we suggest for the  $\text{AlP}_1$  cation species, the intermediate species of the transformation from  $\text{Al}_{13}$  to  $\text{AlP}_2$ . Two heteropoly(oxometallate) anions, namely,  $\text{SiW}_{11}\text{O}_{39}^{8-}$  and  $\text{HPW}_{11}\text{O}_{39}^{6-}$ , have been shown to

(37) Muller, D.; Grunze, J.; Hallas, E.; Ladwig, G. Z. *Anorg. Allg. Chem.* 1983, 500, 90.

(38) Pope, M. T. In *Heteropoly and Isopolyoxometallates*; Inorg. Chem. Concepts, 8; Springer-Verlag: Berlin, 1983.

adopt a similar defect structure, based on the  $\alpha$ -Keggin structure.<sup>39,40</sup> The aluminum analogue, however, would possess a more "open" structure and thus would be expected to be less stable. This is in accordance with our observation of this species as a transient in the aging process. The NMR data for AIP<sub>1</sub> indicates that the loss of the aluminum octahedron results in less distortion of the remaining 11 octahedral sites but increased distortion of the tetrahedral site. Since the defect structure has four new terminal AlOH, which were originally bridging groups in the Keggin structure, condensation of the defect structure via elimination of H<sub>2</sub>O on these sites is the most logical pathway for the formation of the more stable polycation species, AIP<sub>2</sub>.

The bulk of our evidence indicates that AIP<sub>2</sub> is a dimer of the AIP<sub>1</sub> structure. Our GPC measurements, in agreement with those of Akitt on hydrolyzed solutions,<sup>17</sup> show that it is not much larger than Al<sub>13</sub>. Other, more extensive GPC studies have found a species in similar sols that appears to be AIP<sub>2</sub>, which has a molecular weight range of about 1500–3000 Daltons.<sup>8</sup> These data, together with mechanistic considerations and our estimated radius of 7 Å derived from the Stokes equation strongly support our formulation as "Al<sub>24</sub>O<sub>72</sub>". Although <sup>27</sup>Al NMR provides clues as to its molecular architecture, the actual structure determination awaits crystallization of this species. Our efforts to succeed in this endeavor have been so far hindered by the strong tendency of the material to form glasses.

There are several different ways that one can combine two Al<sub>12</sub>O<sub>39</sub> or AIP<sub>1</sub> units (Figure 9b) together. One possible structural model in accordance with the NMR data is shown in Figure 9c. It is well-known that the NMR resonance width of quadrupolar nuclei reflects the symmetry of the coordination environment. For example, the central tetrahedral aluminum in Al<sub>13</sub> has a very symmetric coordination environment. It is bonded to four oxygen atoms, each of which is coordinated to three other octahedral Al atoms. The symmetric environment, in which all of the bond lengths and angles are identical, results in a zero electric-field gradient at the Al nucleus. This accounts for the very narrow resonance observed. On the other hand, in the model proposed for AIP<sub>1</sub> only three oxygen atoms at the tetrahedral site are each coordinated to three octahedral Al atoms. The fourth oxygen atom is coordinated to two octahedral Al atoms (indicated by the circle in the figure). Importantly, the same tetrahedral site asymmetry is preserved in the AIP<sub>2</sub> structure with C<sub>2</sub> symmetry shown in Figure 9c and in another isomer with C<sub>2h</sub> symmetry (not shown). This could account for the broader tetrahedral resonance of AIP<sub>2</sub> (and AIP<sub>1</sub>) compared to that of Al<sub>13</sub>. In contrast, in other possible structures for AIP<sub>2</sub> such as the one shown in Figure 9d, the local environment at the tetrahedral site is the same as that in Al<sub>13</sub>; therefore it is not as likely a model.

Although we are unable to discriminate between these specific structures with the available data, we can make general conclusions about the interpretation of some experimental observations. For example, the NMR spectral changes that have been observed in previous studies of hydrolysis and aging and in aluminum chlorohydrate solutions can be explained on the basis of these models. The greater stability of AIP<sub>2</sub> to attack by acids or ferron can also be attributed to the larger cluster size, higher hydrolysis ratio, and protected tetrahedral Al sites. On the other hand, the equilibrium between Al<sub>13</sub> and the defect

Table III. Integrated Intensities of the <sup>27</sup>Al NMR Resonances for Selected GPC Fractions

fraction	75.6 ppm (AIP <sub>3</sub> )	70.2 ppm (AIP <sub>2</sub> )	62.9 ppm (Al <sub>13</sub> )	0 ppm (Al <sup>3+</sup> )	~10 ppm (oct, total)	O <sub>h</sub> /T <sub>d</sub> ratio <sup>b</sup> (sum of AIP <sub>2</sub> + AIP <sub>3</sub> )
38	0	0	0	65		
40	0	0	0	95		
42	0	0	0	89		
44	0	0	0	74		
46	0	0	0	64		
47	0	0	0	55		
48	7.8	11.1	0	47	190	10.1
49	13.2	46.6	0	32	598	10.0
50	17.6	69.2	0	25	971	11.2
51	15.7	96.3	0	13	1275	11.4
52	13.4	123.3	0	10	1468	10.7
53	9.1	116.4	0	5.3	1359	10.8
54	5.8	111.0	0.4	0	1251	10.7
56	0	88.8	1.1	0	1045	11.6
58	0	58.4	1.7	0	613	10.2
60	0	39.8	2.4	0	468	11.1

<sup>a</sup> Corrected for Al<sub>13</sub> contribution. <sup>b</sup> The octahedral contribution is corrected for the Al<sub>13</sub> contribution as noted in Table II and thus reflects the O<sub>h</sub>/T<sub>d</sub> ratio for AIP<sub>2</sub>, AIP<sub>3</sub>. The average value is 10.8 ± 0.8.

structure (AIP<sub>1</sub>) can account for the fast reaction of Al<sub>13</sub> with acids and ferron.

We do not have enough data to provide a structural model for AIP<sub>3</sub>. The NMR data indicate that the Al environments are similar to AIP<sub>2</sub> and that it follows AIP<sub>2</sub> in the aging process. As the GPC data indicate, it has a higher molecular weight, and it may be a trimer or tetramer of the Al<sub>12</sub>O<sub>39</sub> structure. Recently, both Akitt<sup>17</sup> and Fitzgerald<sup>8</sup> have suggested models for the "70 ppm" species, which have nuclearities of Al<sub>20</sub> and Al<sub>41</sub>, respectively. The former has an octahedral/tetrahedral aluminum ratio of 9 and the latter, 7.2. As we have shown, both of these ratios are too low to describe AIP<sub>2</sub>, although they are similar to the ratio that we have observed for AIP<sub>3</sub> of 8.4. However, the Al<sub>41</sub> model contains two types of tetrahedral aluminum in a 4:1 ratio, in which the unique T<sub>d</sub> site has the same symmetric environments as Al<sub>13</sub>. Therefore, it should give a very narrow resonance line. This structure can be ruled out as a model for AIP<sub>3</sub>. The Al<sub>20</sub> structure is also not a likely candidate for AIP<sub>3</sub> as it would have a (slightly lower) molecular weight and shape, which would probably result in it being indistinguishable from Al<sub>24</sub> by GPC.

We believe that we have uncovered some of the fundamental pathways by which alumina sol species grow and evolve in the early stages of thermal evolution. <sup>27</sup>Al NMR has been particularly important in following the kinetics of the transformation, and GPC has allowed us to isolate the products. This study demonstrates an aging mechanism based on the oligomerization of Al<sub>13</sub>-like units. Our data suggest that the first (dimerization) step arises from recombination of two defect Al<sub>13</sub> structures and points to a formulation of Al<sub>24</sub>O<sub>72</sub> for the dimer. We are currently exploring details of this structure using <sup>1</sup>H and <sup>17</sup>O NMR spectroscopy. Further oligomerization of the "Al<sub>24</sub>" cluster creates another species, AIP<sub>3</sub>, which appears to be larger but whose identity is still unknown. We do not find evidence for this oligomerization occurring on increasing the hydrolysis ratio, but rather on thermal treatment of the clusters. The role of this polymerization in alumina formation is still speculative. It is interesting to note, however, that gels that have a substantial amount of AIP<sub>2</sub> show a NMR resonance in the solid state at 33 ppm after they are heated to 200 °C, which is indicative of either a very unusual tetrahedral Al site or five-coordinate Al.<sup>41</sup> These

(39) Matsumoto, K. Y.; Sasaki, Y. *Bull. Chem. Soc. Jpn.* 1976, 49, 156.

(40) Fuchs, J.; Thiele, A.; Palm, R. *Z. Naturforsch.* 1981, 36b, 544.



are promising first steps on the way to understanding the thermal evolution of alumina sol-gels en route to ceramic materials.

**Acknowledgment.** We thank the Ontario Centre for Materials Research for seed funding for this project (L. F.N.) and NSERC for support via a Strategic Grant and through operating grants (to L.F.N. and A.D.B.). We also

(41) Nazar, L. F.; Fu, G., unpublished results. Wood, T. E., private communication; and see ref 24.

thank Dr. Tim Allman for making NMR-286 available to us. We are grateful to Dr. Brian Sayer and Dr. Don Hugues at McMaster and Janet Venne at Waterloo for their technical NMR assistance.

### Appendix

Integrated intensities of the  $^{27}\text{Al}$  NMR resonances for selected GPC fractions are given in Table III.

**Registry No.**  $\text{Al}_2\text{O}_3$ , 1344-28-1;  $\text{Al}_{13}\text{O}_4(\text{OH})_{24}(\text{H}_2\text{O})_{12}^{7+}$ , 12703-68-3.

## Photophysical and Photochemical Studies of Phenothiazine and Some Derivatives: Exploratory Studies of Novel Photosensitizers for Photoresist Technology<sup>1,†</sup>

Mónica Barra,<sup>2</sup> Gary S. Calabrese,<sup>\*3</sup> Mary Tedd Allen,<sup>3</sup> Robert W. Redmond,<sup>4</sup> Roger Sinta,<sup>3</sup> Angelo A. Lamola,<sup>3</sup> Richard D. Small, Jr.,<sup>3</sup> and J. C. Scaiano<sup>\*2,4</sup>

*Department of Chemistry, University of Ottawa, Ottawa, Canada K1N 6N5; Shipley Company, Inc., 455 Forest Street, Marlboro, Massachusetts 01752; and Division of Chemistry, National Research Council, Ottawa, Canada K1A 0R6*

*Received September 18, 1990. Revised Manuscript Received December 18, 1990*

The photochemistry and photophysics of a series of phenothiazine derivatives have been examined by using a combination of time-resolved laser techniques. The triplet states, which are readily detectable by using laser flash photolysis techniques, decay with lifetimes in the neighborhood of 1  $\mu\text{s}$ ; these lifetimes are frequently influenced by self-quenching processes. All the phenothiazines are modest singlet oxygen sensitizers, with yields,  $\Phi_{\Delta}$ , in the 0.18-0.46 range. The rate constants for the reactions of both singlet and triplet states with bromo compounds correlate well with the free energy for electron transfer. Increased delocalization (e.g., by introduction of naphthalene moieties) shifts the ground-state spectrum to the red so that they show significant absorption at the mercury lamp g line; however, the rate constants for reaction with I (1,3,5-tris(2,3-dibromopropyl)-1,3,5-triazine-2,4,6-(1*H*,3*H*,5*H*)-trione) are reduced to a point where only singlet processes are likely to be of importance.

### Introduction

A number of negative photoresist systems have been reported over the years that involve a variety of insolubilization schemes.<sup>5,6</sup> Photoinduced cross-linking of the matrix polymer is a mechanism often employed in order to achieve differential solubility. In these systems the cross-linker (which may be part of the polymer chain) can be inherently photoactive or it can be activated by another component of the resist. Typical examples include poly(vinylcinnamate) resists,<sup>7</sup> bisazide-based resists,<sup>8</sup> and acid-catalyzed cross-linking systems (e.g., epoxy materials).<sup>9</sup>

Recently, a family of acid-hardened photoresists has been developed. They are comprised of three components; a photosensitive acid generator (PAG), an acid-activated, thermally assisted cross-linker, and a phenolic polymer. The cross-linking chemistry of these systems is related to that found in thermoset coatings.<sup>10</sup> In the first step the resist is exposed and acid is liberated from the PAG. The acid in turn activates a multifunctional cross-linker, which upon heating reacts with the polymeric matrix according to Scheme I.

Two high-resolution negative resists for use with e-beam and deep-UV exposure tools have been reported.<sup>11,12</sup> In addition to having high contrast, these systems exhibit excellent plasma etch resistance and thermal stability.

For certain applications it is advantageous to extend the photosensitivities of all of the aforementioned systems to 365 (i line) and 436 nm (g line), the wavelengths used with conventional diazonaphthoquinone/novolak photoresists. To accomplish this, an appropriate chromophore may be incorporated into the structure of the PAG or, alternatively, by the addition of a photosensitizer capable of activating the PAG. Both of these approaches have been utilized with a variety of PAG molecules. The spectral sensitivity of onium salts has been shifted to longer wavelengths by adding extended aromatic substituents.<sup>13</sup> A wide variety of aromatic sensitizers have also been used in conjunction with onium salts in order to generate acid

(1) Issued as NRCC-32326.

(2) University of Ottawa.

(3) Shipley Co. Inc.

(4) NRCC.

(5) Reiser, A. *Photoreactive Polymers, The Science and Technology of Resists*; Wiley-Interscience: New York, 1989.

(6) Moreau, W. M. *Semiconductor Lithography*; Plenum Press: New York, 1988.

<sup>†</sup>Dedicated to Professor Kurt Schaffner on the occasion of his sixtieth birthday.